


4-2017

Photocontrol of pH via Doped Conjugated Polymer Nanoparticles

Aaron I. Bayles

College of William and Mary

Follow this and additional works at: <https://scholarworks.wm.edu/honorsthesis>

 Part of the [Organic Chemistry Commons](#), [Physical Chemistry Commons](#), and the [Polymer Chemistry Commons](#)

Recommended Citation

Bayles, Aaron I., "Photocontrol of pH via Doped Conjugated Polymer Nanoparticles" (2017).
Undergraduate Honors Theses. Paper 1016.
<https://scholarworks.wm.edu/honorsthesis/1016>

This Honors Thesis is brought to you for free and open access by the Theses, Dissertations, & Master Projects at W&M ScholarWorks. It has been accepted for inclusion in Undergraduate Honors Theses by an authorized administrator of W&M ScholarWorks. For more information, please contact scholarworks@wm.edu.

Photocontrol of pH via Doped Conjugated Polymer Nanoparticles

A thesis submitted in partial fulfillment of the requirement
for the degree of Bachelor of Science in Chemistry from
The College of William & Mary

by

Aaron Bayles

Accepted for _____

Professor Elizabeth Harbron, Director

Professor Robert Hinkle

Assistant Professor William McNamara

Associate Professor Jonathan Arries

April 27th, 2017

Contents

Acknowledgements.....	3
Table of Figures.....	4
Introduction	6
Chapter One: Project Goals and Basis	13
Chapter Two: Dye Doping of PPE Nanoparticles	16
Chapter Three: Nanoparticle Coating.....	21
Chapter Four: Effect of Starting pH	24
Chapter Five: Residual THF	25
Future Direction	28
Conclusion.....	30
Appendix 1 Reprecipitation	31
Appendix 2 Base Release	33
Appendix 3 PVK Nanoparticles	35
Appendix 4 Synthesis	36

Acknowledgements

I'd like to thank **Professor Elizabeth Harbron** for her academic and personal support during my time at W&M. Her guidance has been a critical part of my academic and personal formation here, and has provided me a strong foundation to be a better student and researcher in the future. **I'm also incredibly grateful to Professors Robert Hinkle, William McNamara, and Jonathan Arries** for their part on this committee.

Lastly, I'd like to recognize **Lisa Graves and Tyler Larson** for their outstanding contributions to this research thus far, and for the progress that I know they will make in the future.

Table of Figures

Figure 1 PVK structure

Figure 2 Visualization of reprecipitation procedure

Figure 3 Jablonski diagram, and absorbance/fluorescence spectra of a substance

Figure 4 Visualization of FRET phenomenon

Figure 5 pH scale

Figure 6 Photo-induced activity of reversible and irreversible photoacids

Figure 7 Combination of polymer plus photoacid yields nanoparticle

Figure 8 Representation of actual fluorescence data and what we expect the corollary pH change to be

Figure 9 Structure of poly(2,5-di(2'-ethylhexyl)-1,4-ethynylene)

Figure 10 Fluorescence of PPE nanoparticles

Figure 11 Photobleaching of fluorescence and absorbance of undoped PPE nanoparticles

Figure 12 Molecular structure of photoacid dyes

Figure 13 FRET overlap of PPE with photoacids

Figure 14 Definitions of CPNs and reprecipitation visualization with doping information

Figure 15 Fluorescence modulation, zeta potential change, and pH change of doped α nanoparticles.

Figure 16 Results from β and γ nanoparticle experiments

Figure 17 Comparison of blank and dyed nanoparticles absorbance spectra

Figure 18 Kinetics test at 420nm. Left is blank nanoparticles, right is doped

Figure 19 Molecular structures of poly(allylamine hydrochloride) and polyethyleneimine

Figure 20 Absorption results from coating pre-made nanoparticles with PEI

Figure 21 Absorption results from coating prenano solution with PEI

Figure 22 Zeta potential change of doped γ CPNs upon coating

Figure 23 Summary of coated CPN data

Figure 24 Effects of extreme pH on fluorescence spectrum of doped nanoparticles

Figure 25 Titration of doped (left) and blank (right) nanoparticles

Figure 26 Effect of residual THF on absorption and fluorescence spectra of nanoparticles, as well as acid release

Figure 27 Comparison of fluorescence modulation of nanoparticles created with and without heat

Figure 28 Summary of different types of nanoparticles and results

Figure 29 Molecular structure and photoreaction of photobase

Figure 30 FRET overlap of photobase absorption and PPE fluorescence

Figure 31 Effect of irradiation on photobase-doped CPNs

Figure 32 Nitrobenzaldehyde Structure

Figure 33 Fluorescence of PVK CPNs

Introduction

This honors project is based on the experimental research I have conducted since the beginning of my sophomore year. The original idea for this research was formulated by Christian Chamberlayne '15 and built on his previous work on the functionalization of conjugated polymers. We believed that by using the exciting field of nanotechnology, we could design a tool to reversibly perturb the pH of a solution using only light, and then utilize the fluorescent properties of that system to track that pH change. Precise control of pH is incredibly important in any type of scientific system, and methods to sensitively and efficiently manipulate and track it, using non-invasive methods, are highly sought after by researchers.

The basis of this research is the conjugated polymer nanoparticle (CPN). Polymers are molecules composed of repeating organic units, strung together in long chains. When a polymer is conjugated, that means that the chains contain a series of alternating double and single bonds, called a pi system. This conjugation grants the polymer a variety of unique properties which will be discussed further. An example of a conjugated polymer, PVK (Poly(9-vinylcarbazole)) is shown in Figure 1.

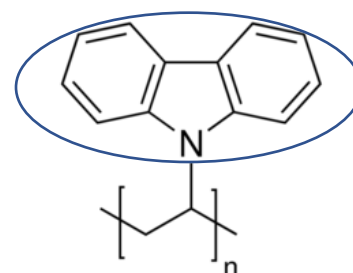


Figure 1 PVK is composed of a saturated backbone with the conjugated substituent circled in blue

The nanoparticles are prepared through a process known as reprecipitation (refer to Appendix 1 for more detailed procedural information). The desired conjugated polymer is dissolved in the solvent THF to create a dilute solution. A fraction of this precursor solution is then injected into a sample of ultrapure water undergoing sonication, distributing the polymer chains throughout the mixture. The THF is then removed via vacuum drying or argon bubbling.

The individual polymer chains, which are not soluble in water, curl onto themselves to create spherical nanoparticles. As a result of the negative surface charge (zeta potential) of the nanoparticles, they repel each other, preventing aggregation. (Figure 2)

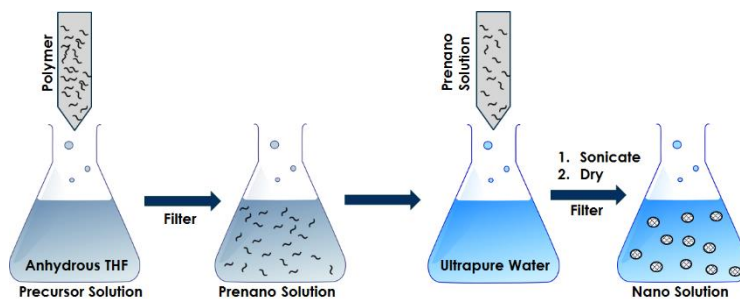


Figure 2 Visualization of reprecipitation procedure

These nanoparticles, like most materials, absorb specific wavelengths of light. This process is defined by the electronic energy levels of the substance. For example, if a particular molecule has an energy gap of 5eV between its ground state and one of its excited states, then only incoming light with an energy of 5eV will be absorbed, temporarily pushing the molecule into an excited state and the electron into a higher energy orbital. This process, absorption, is modeled as the purple arrow in the Jablonski diagram shown in Figure 3a. Within each energy level, there also exist a series of vibrational energy levels that correspond to slightly different energies than the base electronic state, and it is possible for an electron to be excited to any of those sub-levels. As a result, in a graph that plots the absorbance by a substance at any given wavelength, the absorbance values would be represented as a broad peak, rather than a single line at one wavelength. This is shown as the blue line in Figure 3b.

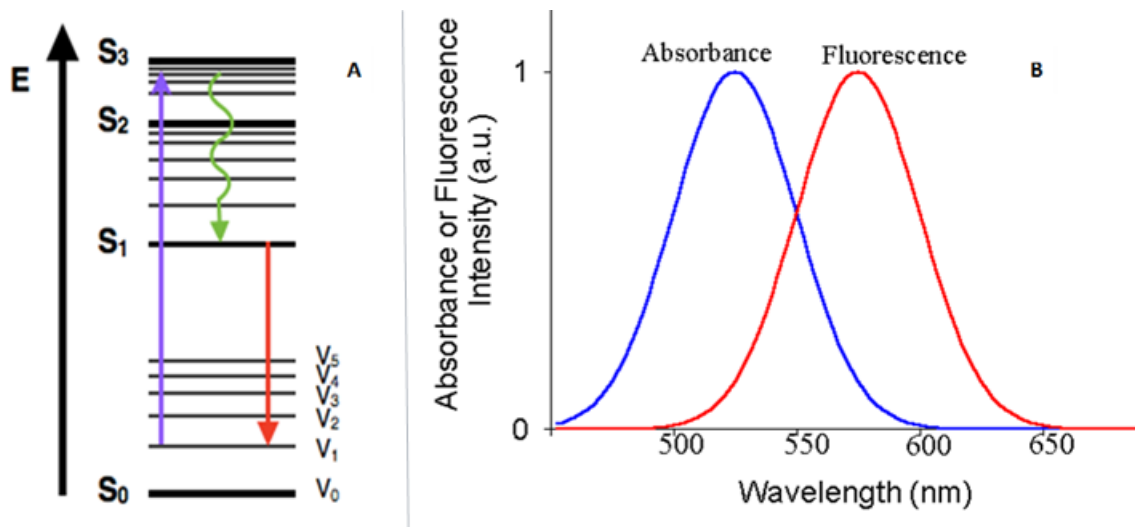


Figure 3 The left image is a Jablonski diagram, a representation of electronic energy levels. On the right are the absorbance and fluorescence spectra of a substance

In dilute solutions, the amount of light absorbed by the dissolved molecule is proportional to the concentration of that molecule. This intuitively makes sense. If I imagine that we are gradually adding dirt to a glass of clear water, the more dirt I add, the more opaque the liquid will become. This same principle can be applied to calculate the concentration of molecules within a solution, assuming I know the molecule's inherent absorptivity, or its "opaqueness." This is known as Beer's Law and is expressed by the equation

$$A = \epsilon bc$$

where A is absorbance, ϵ is the molar absorptivity of the substance (an intrinsic property of all substances), b is the cell length, and c is the concentration of the molecule. Additionally, changes in the UV-vis absorption spectra can provide insight into the invisible processes at play on the nano level. For example, successive absorption tests can be used to track the progress of a reaction, as peaks from starting materials decrease relative to peaks attributed to products.

In many cases, once an electron has been excited to a higher energy state, it will eventually return to the ground state via a non-radiative transition, releasing energy as heat or

kinetic energy. However, another option exists, fluorescence. In this process, after the electron is excited to a high vibrational level within an energy level, it releases some of that energy to drop to the lowest energy vibrational state (represented by the green arrow in Figure 3a), before dropping once again to the ground state and releasing energy in the form of light. This process is represented in Figure 3a by the red arrow. As a result of that relaxation stage, the energy of the emitted light is lower, and therefore its wavelength is longer than that of the excitation light, shown in Figure 3b. This phenomenon is known as the Stokes Shift and is observed in all fluorescent materials.

It must be noted, however, that fluorescence does not occur in all substances. The non-radiative transition is normally significantly faster than the emission transition, meaning that there is simply no time for the fluorescence to occur before the electron returns to the ground state. As such, certain conditions must be fulfilled to make the fluorescence process more favorable.

One property that the polymers used in this research derive partly from their conjugation and planarity is the ability to fluoresce. Long conjugated backbones can act as fluorophores, capable of absorbing and emitting light. The CPNs have a relatively good quantum yield, meaning that the fluorescence pathway is favored, due to the large number of fluorophores in a small space, resulting in a very intense fluorescence.¹

Absorption and fluorescence information is very useful for a variety of purposes, and when used in conjunction, the utility of these processes further increases. Förster Resonance Energy Transfer (FRET) is a phenomenon that can occur when the fluorescence spectrum of one molecule (the donor) overlaps with the absorbance spectrum of another molecule (the

acceptor). When this condition is met, and the two molecules are in close proximity, excitation of the donor can result in the nonradiative excitation of the acceptor molecule. This occurs because the process of energy transfer is faster than that of fluorescence. To better understand the results of this process, let us envision a two-molecule system where one molecule absorbs blue light and fluoresces green, while the other molecule absorbs green light and fluoresces red light (Figure 4a). If FRET occurs between this pair, then irradiation with blue light will result in the emission of red light. The FRET efficiency is dependent on distance, as demonstrated in the following equation

$$E = \frac{1}{1 + \left(\frac{r}{R_0}\right)^6}$$

where E is the FRET efficiency, r is the distance between the donor and acceptor molecules, and R_0 is the Förster radius, the distance at which FRET efficiency is 50%. As such, FRET can be used as nanoscale ruler, measuring the distance between molecules by measuring the light emission.

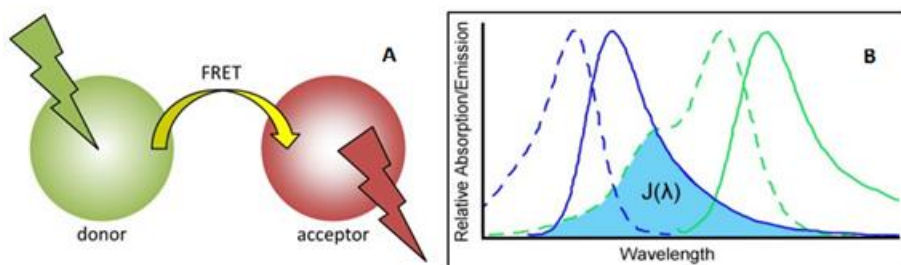


Figure 4 Visualization of FRET phenomenon². A represents energy transfer between molecules, B shows the overlap of their spectra.

However, FRET can manifest itself in a variety of ways. For example, if the acceptor in the above FRET pair does not fluoresce, then it will have a quenching effect on the donor molecule, decreasing the expected green fluorescence. Additionally, an interesting effect can arise in a system where there are multiple donor molecules per acceptor molecule. In this

situation, the donor molecules act like a magnifying glass or antenna, focusing the energy onto the acceptor, increasing the efficiency of the energy transfer between the molecules. In this case, the FRET process is actually more efficient than if the acceptor molecule were to be directly irradiated from an outside source.

Another essential concept to this research is pH, which is the measure of hydrogen/proton concentration within a cell. The proton is a fundamental and ubiquitous catalyst, and the role of proton concentration in analytical solutions has far-reaching effects. It is expressed in a negative logarithmic scale, from 0-14, in which a low number denotes a high proton concentration. A visualization of the pH scale is given below, with some example of common materials and their pH. Slight changes in pH can dramatically alter reaction kinetics, formation of byproducts, and other chemical traits. As such, the control of proton concentration and transfer is among the most important processes in science.

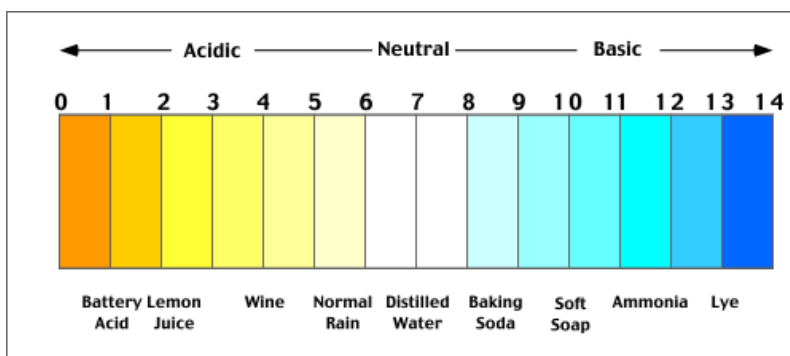


Figure 5 pH scale

Photoacids are molecules that convert into a more acidic form upon irradiation with specific wavelengths of light. This can happen either reversibly or irreversibly, depending on the exact reaction to light stimulus. For example, the irradiation of nitrobenzaldehyde results in an irreversible rearrangement that results in the ejection of an acidic proton. Merocyanine-

derivatives, on the other hand, undergoes a reaction that releases a proton under irradiation with visible light, which undergoes complete reversal when the light source is removed³.

Importantly, most useful photoacids are insoluble in water.

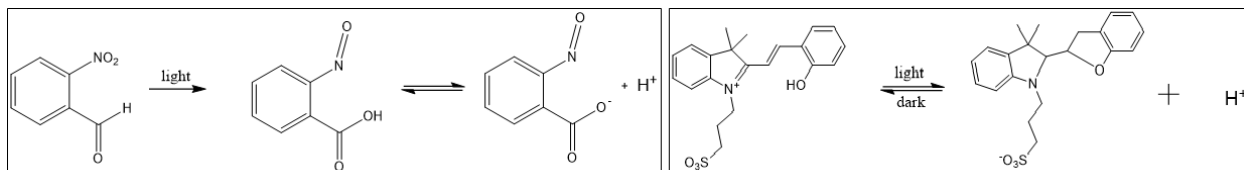


Figure 6 Photo-induced activity of reversible and irreversible photoacids

By themselves, photoacids have already demonstrated a wide range of applications. For example, they have been shown as a potential tool in the fight against multi-drug resistant bacteria⁴, as well as an important catalyst in supramolecular self-assembly⁵. They have even shown utility in the optimization of microbial fuel cells⁶ and efficient building of nanomachines⁷. Manipulation of proton concentration within a system via light is a powerful function. However, I believe that researchers are only just beginning to tap the full potential for these molecules.

For this honors research, I have sought to create a tool that can reversibly change the pH of an aqueous solution in response to light. My goal was to use a FRET pair of a conjugated polymer nanoparticle (donor) and a photoacid (acceptor) to create a water-compatible system that efficiently releases acid upon irradiation with UV light via the antenna effect, and reabsorbs that acid when the light source is turned off. Furthermore, I used photoacids that are quenching in their ground state, but are non-quenching in their excited, acid-releasing state. As such, the pH change could be tracked by monitoring the change in fluorescence and correlating that to the amount of acid release.

Chapter One: Project Goals and Basis

This experiment began during my time with Christian Chamberlayne. The aim was to use a PPE-derived polymer, poly(2,5-di(2'-ethylhexyl)-1,4-ethynylene) doped with 2-hydroxyazobenzene photoacidic dyes, THOMeCl₃ and THSMeCl₃, to make a nanoparticle tool that would accomplish our goals of reversible acid release and simultaneous fluorescence modulation (visualized in Figure 7). With those two criteria achieved, it would be possible to create a model to track acid release via the fluorescence (refer to Figure 8 for ideal data).

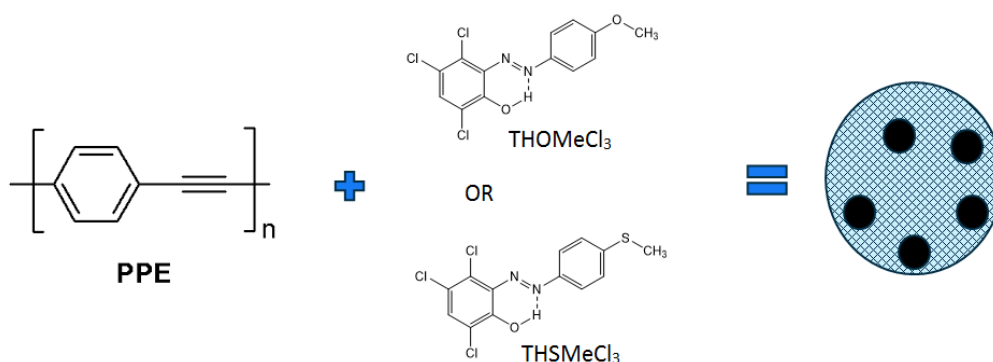


Figure 7 Combination of polymer plus photoacid yields nanoparticle

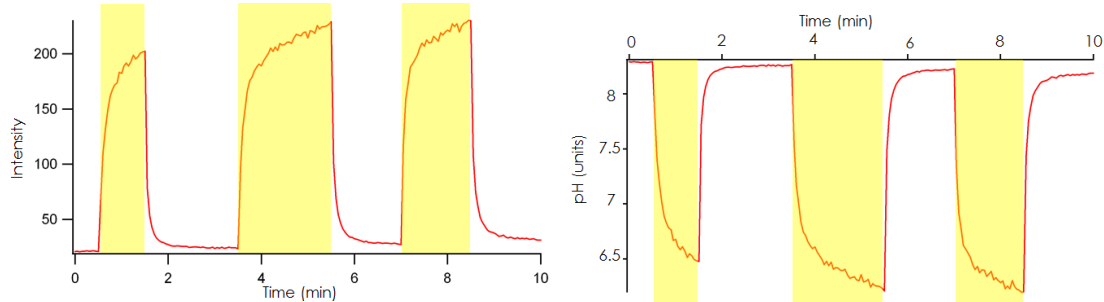


Figure 8 Representation of actual fluorescence data (left) and what we expect the corollary pH change to be (right). The pH data was created by inverting the fluorescence data and updating the y-axis. Yellow rectangles represent irradiation periods.

Shown here, this PPE derivative contains a planar conjugated backbone and two saturated sidechains that result in a very high intensity fluorescence ($\phi_f = 0.12$)⁸ with λ_{\max} at approximately 420nm, creating a bright royal blue color (Figure 10). This is ideal, as a large natural fluorescence is a critical foundation for our nanoparticle to have in order to detect fluorescence modulation later. However, PPE is also highly susceptible to photobleaching, photo-induced damage, which manifests as an irreversible increase in the fluorescence of the nanoparticle and a permanent decrease in the absorption, as seen in Figure 11. Too much photobleaching would greatly diminish our ability to calculate the amount of acid released into solution via fluorescence alone.

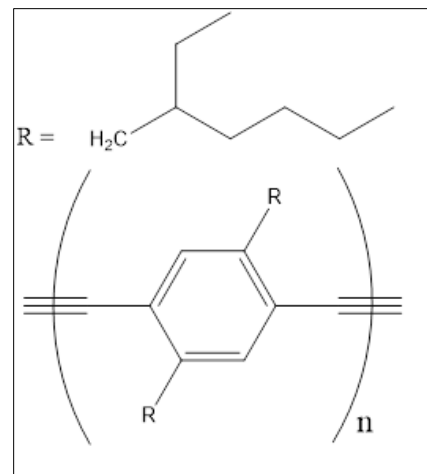


Figure 9 Structure of poly(2,5-di(2'-ethylhexyl)-1,4-ethynylene)

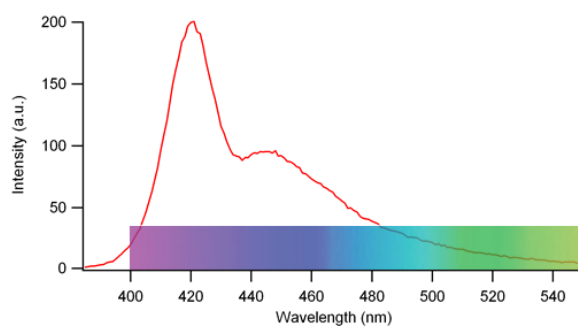


Figure 10 Fluorescence of PPE nanoparticles

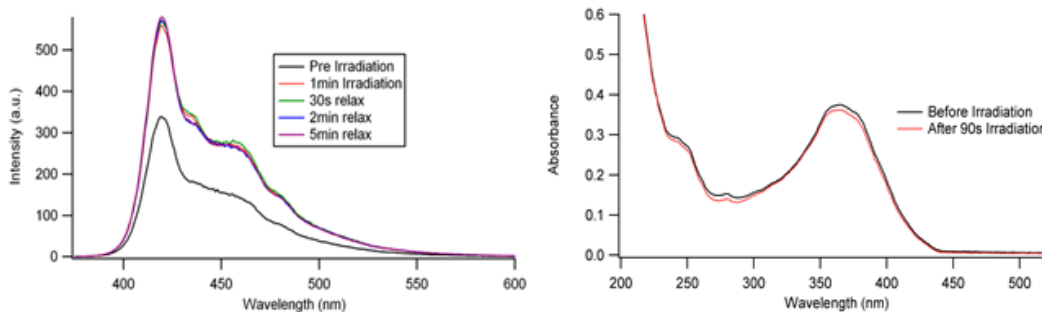


Figure 11 Photobleaching of fluorescence and absorbance of undoped PPE nanoparticles

The two different photoacid dyes used in this experiment were synthesized in our lab (See Appendix 4) and characterized previously⁹. Upon excitation, they undergo a trans-to-cis isomerization via a rotation around the nitrogen-nitrogen double bond. This breaks the hydrogen bond that the phenolic hydrogen had with the nitrogen, increasing the acidity of the molecule and the ability for the proton to be released into solution. When the excitation source is removed, the molecule reabsorbs any released protons and returns to its more thermodynamically stable trans configuration, reestablishing the hydrogen bond and causing the pH of the solution to revert to pre-excitation levels. Both of these dyes have previously been used to reversibly manipulate pH before, but only in mixtures of water and acetonitrile, as they are not soluble in water alone. As such, they are unsuitable for use in biological environments and most real-world situations.

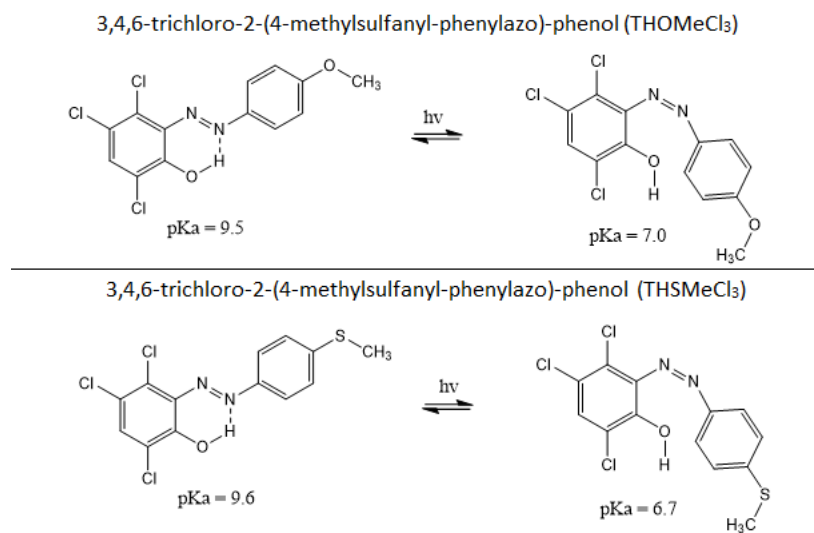


Figure 12 Molecular structure of photoacid dyes

The FRET overlap between the PPE and both of the photoacids is exceptionally large, signifying that energy transfer is likely and should hypothetically be a high-efficiency process (Figure 13). Furthermore, the photoacids utilized undergo a reversible acid release process and

are resistant to photo-induced damage, meaning that they can be used over numerous cycles without decay. As a result of the FRET process, the photobleaching of the polymer itself would also be greatly reduced, but not necessarily eliminated.

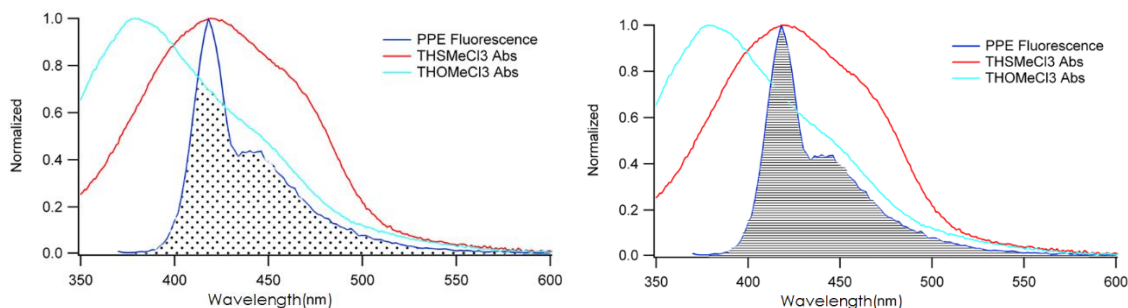


Figure 13 The left image shows the FRET overlap of PPE with THOMeCl₃, while the right shows the overlap of PPE and THSMeCl₃

Chapter Two: Dye Doping of PPE Nanoparticles

To incorporate the photoacid into the PPE CPNs, a solution of the dye dissolved in THF was injected into the nanoparticle solution during the reprecipitation procedure. The exact circumstances of the doping, as well as the exact method used for drying, have proven to be the most important independent variables in this experiment, though this project contains a plethora of other factors worthy of investigation. I tested three different methods of doping, which resulted in three distinct types of nanoparticles: α , β , γ CPNs.

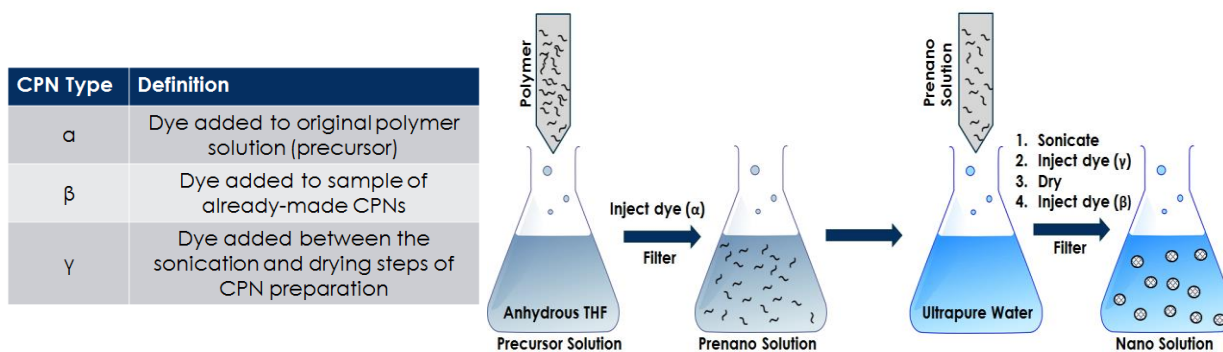


Figure 14 Definitions of CPNs and reprecipitation visualization with doping information

From the project's inception, I have created our doped nanoparticles by injecting the photoacid dye into the precursor solution (the first solution of conjugated polymer dissolved in THF), before any filtration or sonication, hereafter referred to as α nanoparticles. I predicted that this was the best way to incorporate the highest possible amount of dye molecules into the particle and to foster the maximum proximity of the dye to the polymer, creating the most conducive environment for FRET, and therefore, acid release. I found the opposite to be true. Nanoparticles doped with this method exhibited extremely good fluorescence modulation, some photobleaching, and no detectable acid release (Figure 15). At first, I believed these problems stemmed from the negatively-charged polymer absorbing the positively-charged acid upon release. However, measurements of zeta potential of the nanoparticles revealed minimal change after irradiation, indicating that very little acid was actually released.

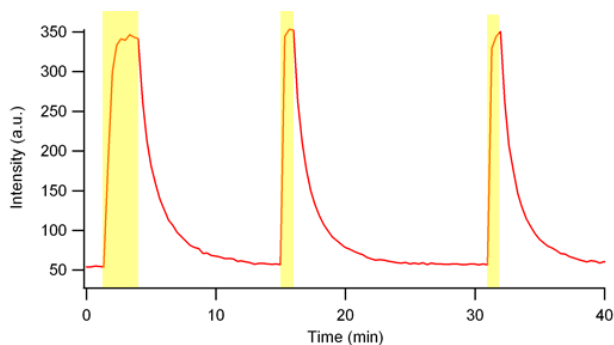


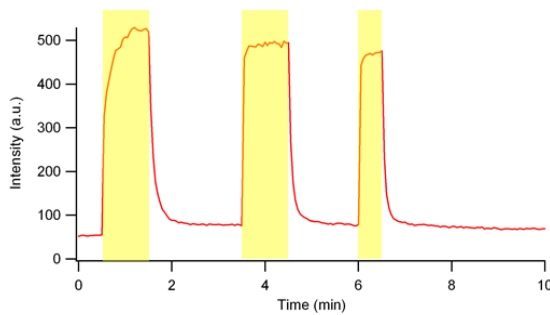
Figure 15 Fluorescence modulation, zeta potential change, and pH change of doped α nanoparticles. Yellow rectangles indicate irradiation.

Zeta Potential Change of Doped α Nanoparticles	
Pre-irradiation	Post-irradiation
-31mV	-32mV
pH Change of Doped α Nanoparticles	
~.02	
Fluorescence Modulation	
~7-20x	

The azobenzene dye molecules appear to exhibit a photomechanical effect, meaning that they physically change shape upon excitation. When nanoparticles were doped during the precursor stage, the dye molecules were dispersed throughout the entire particle, with the majority of them on the inside. However, because of this photomechanical effect, steric

hindrance from the bulky polymer chains have the potential to prevent the dye molecule from undergoing the bond rotation that would result in a conformation more favorable for acid release. As such, the dye molecules within the nanoparticles exercised a quenching effect on the fluorescence, but did not have the ability to isomerize and thereby release acid and modulate fluorescence. Furthermore, they still underwent FRET, essentially stealing that energy from the photoacids on the surface of the particle and quenching the fluorescence of the nanoparticle.

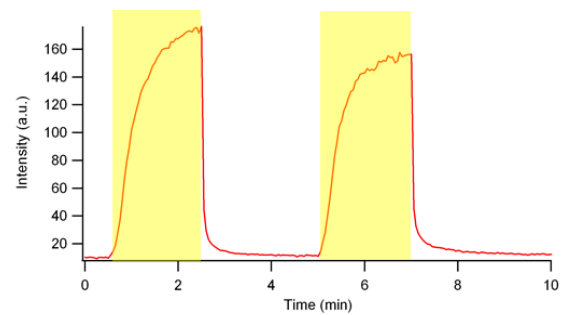
To solve this problem, I experimented with different ways to maximize the number of azobenzene molecules on the surface of the molecule, while minimizing the number on the inside. This primarily involved adjusting our procedure by changing when I injected the dye solution. I found that while adding the dye immediately either before or after removing the THF both resulted in highly successful fluorescence modulation and only a small amount of bleaching, injecting the dye between the sonication and drying steps resulted in nanoparticles that released a significant amount of acid. (Figure 16). Zeta potential measurements of these nanoparticles also showed a significant increase in charge, signifying that acid had been released, and that some of it had been absorbed by the polymer. From this stage, our goal became to minimize the amount of acid absorbed by the nanoparticles and to achieve reversibility.



pH Change of Doped β Nanoparticles per irradiation cycle

~.03

Figure 16 Results from β and γ nanoparticle experiments



pH Change of Doped γ Nanoparticles per irradiation cycle

~.22

Zeta Potential Change of Doped γ Nanoparticles (mV)

Pre-irradiation	Post-irradiation
-39.3mV	-36.91mV

The first step was to measure how much of the dye was isomerizing from the trans to cis form using UV-Vis absorption. Based on that

observation, I could calculate the expected pH change in order to better gauge exactly how much acid was being absorbed by the polymer. Initially, I measured absorption spectra of samples of doped and undoped nanoparticles. I then subtracted the blank, normalized spectrum from the dyed spectrum, leaving me with a difference spectrum that reflects only the photoacid molecules, from which the concentration of the dye can be extracted.

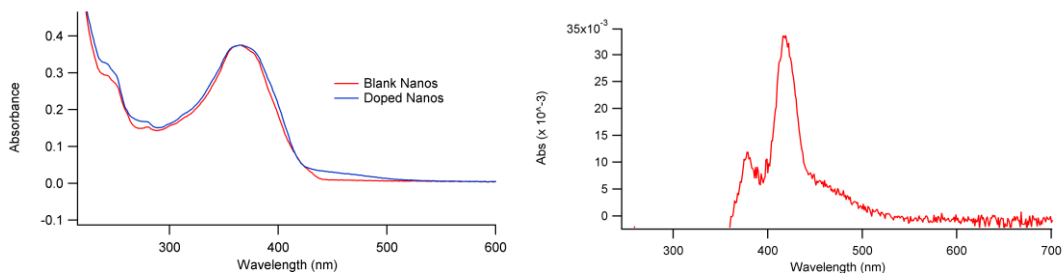


Figure 17 Comparison of blank and dyed nanoparticles absorbance spectra

Next, I performed an absorption kinetics test on the blank sample, nanoparticles without any photoacid attached, detecting the absorbance at a single wavelength (420nm, the

λ_{max} of the dye) as a function of time. Upon irradiation, the absorbance decreased, a result of photobleaching. I know this because when the light source was removed, the absorbance did not return to pre-irradiation levels (Figure 18).

I compared this to the same experiment conducted on a doped sample of nanoparticles. I irradiated the sample and observed that under irradiation the absorbance decreased, and then increased once the light source was removed, though never fully returning to the original absorbance. This was observed over numerous cycles (Figure 18). The cis (photogenerated) form of the photoacids has a lower extinction coefficient than the trans (stable) state, meaning that as the dye switches, I should see its absorbance decrease⁶. The dye also undergoes some photobleaching, though it is far more resistant to it than the polymer. Therefore, based on that information and the results of the kinetics experiment on the blank sample, I believe that the decrease in absorbance observed during irradiation is a combination of photobleaching of both the polymer and the dye, and, more importantly, the switching of the dye. However, because photobleaching is an irreversible process and the photoswitching is reversible, I assumed that the recovery observed once the light was removed only reflected the switching of the dye. Using Beer's Law, I calculated that about 8% of the dye was switching. Using that information, I further calculated that in a 3mL sample, like those I use for the pH tests, I should see a pH change of about 1-2 units, depending on the starting pH. Instead, the highest change we ever observed was .2 units. As such, the next goal for this project was two-fold: to prevent the absorption of acid by the polymer and increase the amount of dye switching.

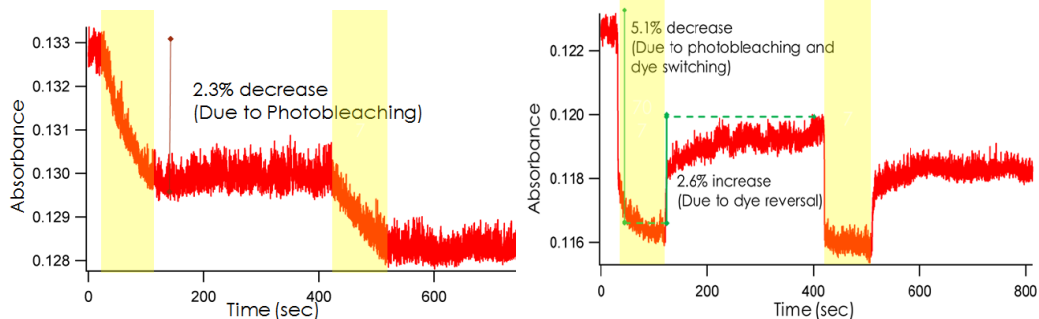


Figure 18 Kinetics test at 420nm. Left is blank nanoparticles, right is doped

Chapter Three: Nanoparticle Coating

In order to maximize the amount of released acid I turned to incorporating positively-charged coating polymers. By coating our nanoparticles with these substances, I hoped to flip the zeta potential of our nanoparticles from negative to positive, thereby decreasing the likelihood that the positively-charged protons released by the photoacids would be absorbed by the polymer. The polymers that I used were polyethyleneimine, or PEI, and poly(allylamine hydrochloride), or PAH. Both of these molecules have been used previously to coat other types of nanoparticles.^{10,11}

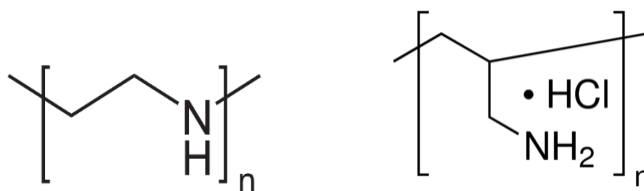


Figure 19 Molecular structures of polyethyleneimine on left and poly(allylamine hydrochloride) on right

I first attempted to use PEI. Little information exists on the exact amounts and proportions of this polymer utilized to coat nanoparticles in previous applications, so I

attempted a variety of procedures. I began by injecting a sample of diluted PEI in H₂O into a sample of previously-made nanoparticles. I then sonicated the sample to attempt to prevent aggregation and distribute the coating polymer evenly among the nanoparticles, and then filtered to remove aggregates. However, all of the nanoparticles aggregated and filtered out of the solution, as demonstrated by absorption scans which showed no or little presence of nanoparticles.

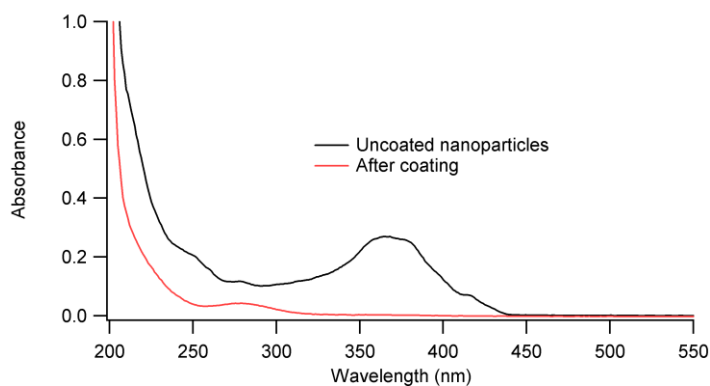


Figure 20 Absorption results from coating pre-made nanoparticles with PEI

Next, I attempted to inject PEI into our prenano solution of our reprecipitation procedure. This also proved completely unsuccessful, as any amount of PEI I added resulted in the complete or near-complete aggregation of the nanoparticles. Even when some nanoparticles remained suspended in the solution after coating, they did not demonstrate any pH change upon radiation and I determined that this was likely due to the very low concentration of the nanoparticles.

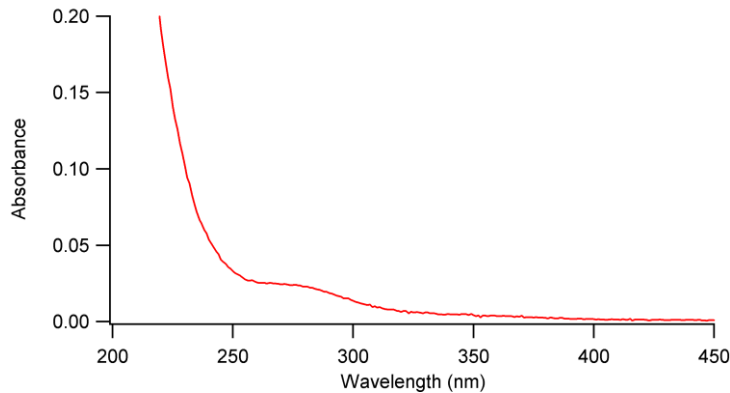


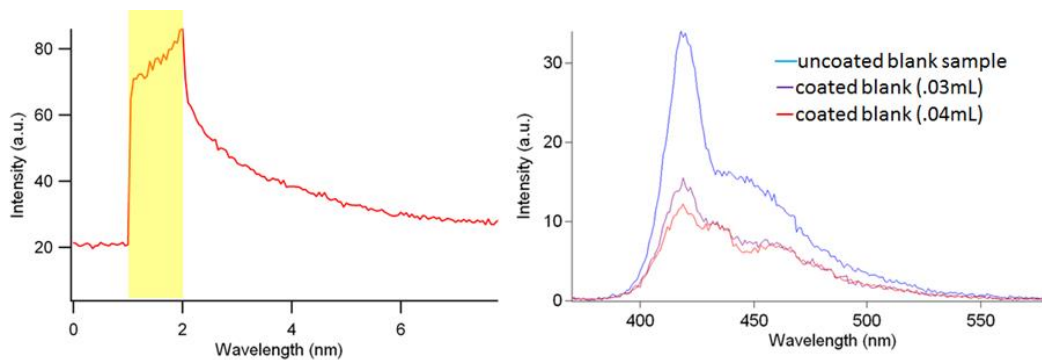
Figure 21 Absorption results from coating prenano solution with PEI

My work with PAH proved much more promising. Our procedure consisted of injecting a dilute water solution of PAH and NaCl into a γ nanoparticle sample and waiting 20 minutes. The nanoparticles did not aggregate, and based on zeta potential data (Figure 22), we achieved our goal of flipping the charge of the nanoparticles from negative to positive.

Zeta—uncoated	Zeta—coated
-31.99mV	22.82mV

Figure 22 Zeta potential change of doped γ CPNs upon coating

Upon coating, I noticed that the fluorescence spectrum changed significantly: decreasing in intensity, and several new peaks appeared. Kinetics experiments also showed that fluorescence modulation had decreased significantly. Finally, a pH test showed that while acid release appeared to occur, it was irreversible and of a lower magnitude than the acid release observed from uncoated nanoparticles. I assume that the coating interfered with the ability for the photoacid molecules on the surface of the nanoparticle to isomerize, resulting in these effects. I have not yet formulated a way to test this hypothesis, or solve the problem, but coating the nanoparticles with PAH proved promising enough that it merits further research.



Fluorescence Modulation
~4x

pH Change of Coated & Doped γ Nanoparticles per irradiation cycle
~.10

Figure 23 Summary of coated CPN data

Chapter Four: Effect of Starting pH

In order to further maximize the acid release observed during the procedure, I experimented with the effect of changing the starting pH before irradiation. I theorized that, based on Le Chatelier's Principle, the photoacid would be more prone to release its hydrogen in

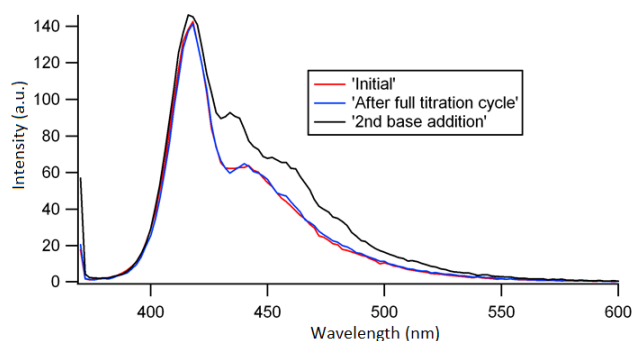


Figure 24 Effects of extreme pH on fluorescence spectrum of doped nanoparticles

a high pH solution. Additionally, because pH is based on a negative logarithmic scale, the same amount of proton added to a basic solution will have a greater effect on the pH than if added to a more acidic solution.

This theory has not yet yielded any improvements in our acid release. In my tests, I executed the irradiation procedure on fresh nanoparticle samples with incrementally increased

starting pHs. Unexpectedly, I found that our pH change did not improve, and at a certain point, the observed pH change decreased instead. Fluorescence tests revealed that addition of base caused the fluorescence of doped nanoparticles to increase significantly, whereas that of undoped nanoparticles remained nearly unchanged, increasing very slightly (Figure 25). This indicates to us that the added base is reacting directly with photoacid, deprotonating it so that when I do irradiate, there are fewer dye molecules that can release acid. Additionally, after reaching a pH threshold of approximately 10.5, the fluorescence and absorption spectra of the doped nanoparticles changed significantly upon return to the starting pH state (Figure 24). I interpret that to mean the nanoparticles are susceptible to decomposition at extreme pH levels, and that there is a limit to how basic I can make the solution before the nanoparticles become unviable for use.

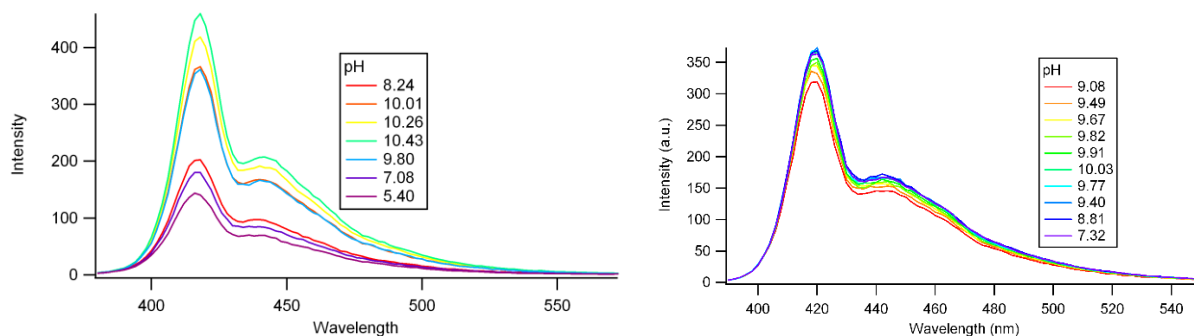


Figure 25 Titration of doped (left) and blank (right) nanoparticles

Chapter Five: Residual THF

I often observed that the presence of THF in the final solution could lead to noticeable changes in the absorption and fluorescence spectra. This normally preceded poor pH results (Figure 26). Since I began working on this project, I have used vacuum drying as the primary

method of removing THF from our prenano solutions, but that comes with some inherent problems. First, evaporative cooling that occurs as a direct result of the procedure can cause the solution to become very cold, even to the point of freezing. This decrease in temperature decreases the kinetic energy of the nanoparticles and increases the possibility of aggregation, resulting in the amassed products filtering out of solution. Additionally, day-to-day changes in the strength of the vacuum have made it difficult to create a consistent system to judge when the solution is actually THF-free, and extended time on the vacuum will also result in some aggregation, leaving us with a smaller concentration of particles in the final solution.

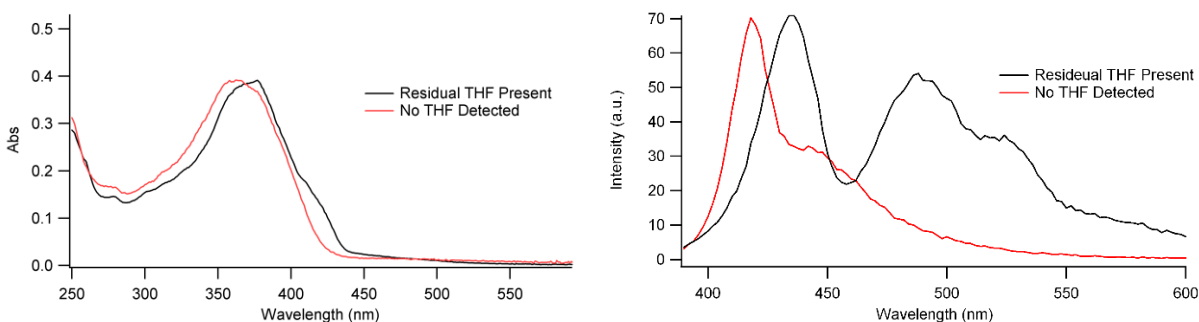


Figure 26 Effect of residual THF on absorption and fluorescence spectra of nanoparticles, as well as acid release

pH Change of Doped γ Nanoparticles with residual THF per irradiation cycle

~.02

As a way to resolve these problems, I have recently turned to a new method of THF removal—argon gas bubbling. Rather than rely on a harsh vacuum to remove the unwanted THF, inert argon is pumped into a round bottom flask containing the post-sonication solution of polymer and dye, which pushes the more volatile THF out of solution. This is a much gentler procedure than the vacuum drying, and does not exercise a potentially destructive cooling effect on the solution. Additionally, because the exact amount of gas pumped into the flask can be sensitively controlled by a flow meter, it is a much more

consistent process which occurs on about the same time scale as vacuum drying, even faster if low-to-medium heat is applied.

This method has proven more consistent than vacuum drying, but has not yet improved positive pH results. We continue to see some irreversible pH change (~ 0.1) which is significant, but no better than what was observed from nanoparticles that were created via vacuum drying. Fluorescence data has been promising, but we have noted that when medium heat is applied (50°C) the nanoparticles become significantly less bright and more susceptible to photobleaching (Figure 27). No pH change was observed in such nanoparticle samples, so recent experiments have been conducted using low heat or none at all.

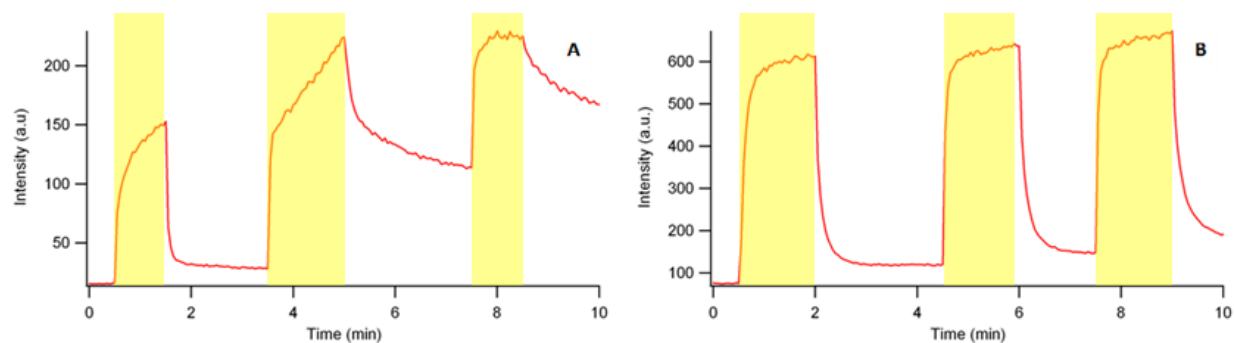


Figure 27 Comparison of fluorescence modulation of nanoparticles created with heat and without heat

Drying Method	Dye addition	Acid Release?	Reversible?	Fl mod factor	Photobleaching	Zeta potential change
Vacuum	α	No	Negative	5-20x	Low	Negative
	β	No	Negative	6x	Moderate	—
	γ	Yes	Partial	7-17x	Moderate	Positive
	γ (coated)	Yes	Negative	4x	Low	—
Argon bubbling	γ (Heat)	No	Negative	4x	High	—
	γ (No heat)	Yes	Negative	7x	Low	Positive

Figure 28 Summary of different types of nanoparticles and results

Future Direction

This project has succeeded in demonstrating that doped nanoparticles have the potential to be effective tools for pH manipulation and monitoring. Some acid release has been detected, and the fluorescence modulation that I have observed is incredibly promising. However, further optimization and improvements to consistency are critical for the eventual practical application of these systems.

While I have shown that moderate pH change using azobenzene-doped PPE nanoparticles is possible, there are several more paths of investigation that this project can take. First, I recommend the exploration of new dye-polymer FRET pairs. In particular, I believe that the PPE I use has been the source of many of our problems, and its affinity for acid is difficult to overcome. Finding a different polymer that is just as fluorescent and absorbs in a similar wavelength range as PPE, but is less negative may allow for more effective acid release.

Second, more work should be done with coating the nanoparticles. This could serve the dual purpose of optimizing the amount of acid reaching solution and protect the nanoparticle from photobleaching. Wrapping the nanoparticles, as opposed to directly coating them, is another option that merits further exploration. This would adjust the zeta potential of the nanoparticles without creating another barrier to prevent effective acid release.

Next, I believe that photobase-generating nanoparticles, as opposed to our photoacid generators, (refer to Appendix 2), created using our new procedure, may succeed where those created using the old procedure did not. By new procedure, I am specifically referring to the addition of dye immediately before drying occurs, as opposed to injection into the prenano

solution. Even a small amount of base release would be a significant step in the functionalization of these nanoparticles, and would further prove that the exact point at which dye is added to the solution is critical to the success of the nanoparticles.

Finally, more sensitive methods should be investigated to monitor pH. The conventional pH probes I have used are simply not designed to measure pH on this scale and are not acceptably reliable for the purposes of this experiment. Due to the physical design of the probes, they are susceptible to inaccurate readings during irradiation by UV light, affecting my ability to trust the output results. Specifically, irradiation of the probe in ultra-purified water showed a modulation of pH consistent with small-scale acid release. While the effect was small, it was not consistent between samples and proved difficult to factor in to our conclusions.

As such, I propose that future researchers should explore the possibility of using fluorescent probes in our nanoparticle solution to monitor pH change more sensitively and with a lower potential for interference. In order for that to be successful, a molecule should be used that undergoes a change in fluorescence in response to changes in pH. This is moderately problematic in our system, however, because the nanoparticles are already fluorescent and finding a probe that will work in the designed wavelength range, while not interfering with the absorbance and fluorescence of the nanoparticles, is difficult.

Conclusion

As the project stands, we have observed the most success with γ nanoparticles dried via vacuum. Much work still needs to be done in order to optimize the system to a point where it is useful in real-world applications, but the foundations have been laid for significant progress in the near future.

It is important to note that while much has been accomplished with this project, there have been times that inconsistencies and unexplained phenomena prevented progress. Contamination of anhydrous THF often resulted in repeated experiments where nanoparticles exhibited undesirable properties (such as altered absorbance or fluorescence spectra) or simply filtered out entirely. Additionally, I still have not come to fully understand how the presence of microscopic amounts of THF in our final solution impact the nanoparticles in terms of their size, charge, fluorescence, susceptibility to photobleaching, and acid-releasing properties. In fact, the nanoparticles themselves are affected by such a wide range of factors that consistently creating nanoparticles with similar properties has been a struggle for the entire duration of this project. However, a significant portion of my time working on this project has been spent troubleshooting problems of this nature, and now that many of them have been solved, the project is poised for a leap forward.

Appendix 1 Reprecipitation

This appendix contains the detailed reprecipitation procedure conducted to prepare our CPNs.

First, prepare the precursor solution. This entails stirring a 1 mg/mL solution of polymer in anhydrous THF under argon atmosphere in the dark for at least 2 hours. This is to ensure that the polymer is fully dissolved. Prepare a 40 ppm prenano solution of conjugated polymer in anhydrous THF by injecting precursor solution into 4.8 mL of THF. Keep stoppered or under Ar_(g)

Next, Prepare 1 mg/1mL solution of dye solution in amber vial. (α only) Add dye molecule to the solution. (Optional) Add a coating polymer.

Filter the solution with .7 μ m filtration paper using the microfiltration set up to remove potential aggregates.

Place 8mL of ultrapure water in a 25 mL round bottom flask. Rinse the graduated cylinder and round bottom with ultrapure water first. Clamp the 25 mL round bottom flask of ultrapure water into the sonicator. To have adequate sonication of the sample during sonication, ensure that the sonicator is at the proper operating level, and the round bottom is centered in the sonicator and at least halfway submerged in the sonicator bath.

Turn on the high vacuum now (there will not be enough time later)

Sonicate the round bottom for 30 sec.

Using a micropipette, transfer 1 mL of prenano solution into the round bottom with the sonicator still on. Do this quickly. Sonicate the sample for 2 min. (γ only) After sonicator is turned off, add dye molecule to the solution. Remove the sample and transfer to the high

vacuum or Ar_(g) bubbling apparatus to remove the THF, as quickly as possible. The polymer will begin to aggregate immediately once the sonicator is turned off.

Next, THF is removed by either vacuum removal or argon bubbling.

For vacuum removal, place a room temperature bath of water on round bottom containing the nanoparticles while they are on the high vacuum. This prevents the solution from freezing from evaporative cooling. There will initially be a large amount of bubbling from the solution. Adjust valves to keep the bubbling consistent, but not intense enough to bump the solution into the upper parts of the vacuum line. Check for THF after 25 min via smell. If THF smell is present, put back on vacuum until no smell is detected. The solution should be clear. Cloudiness is caused by aggregates, but the solution may yield some usable product after next filtration step.

For argon bubbling, place prenano solution into an amber vial. Insert metal needle on gas line into the vial, with the needle clamped above, and the tip of the needle slightly above the bottom. Adjust bubbling rate so that bubbling is constant, but none of the solution bubbles out of the vial. Check for THF after 30 min via smell. If THF smell is present, put back on bubbling apparatus, until no smell is detected. (β only) Add dye molecule to the solution. Proper amount varies by experiment. Filter the nanoparticles with a .7 and .22 μm filtration paper using the microfiltration set up. The solution should be clear after filtration. You can use the 365 nm wavelength on the light source to check for fluorescence of the nanoparticles. (Optional) Add a coating polymer.

Appendix 2 Base Release

In the course of this project, I took a summer-long detour to explore the option of using a photobase dye, in place of the photoacid dye. This was motivated by our theory that the negatively-charged polymer was absorbing the positively-charged protons released by the photoacid dye as a result of electrostatic attraction. Christian Chamberlayne hypothesized that by using a photobase, we could avoid this problem entirely because the negatively-charged base would be repelled by the polymer.

I synthesized the photobase, (*E*)-*N*-cyclohexyl-3-(2-hydroxy-5-nitrophenyl)acrylamide (full procedure in Appendix 4).¹² This particular dye has a

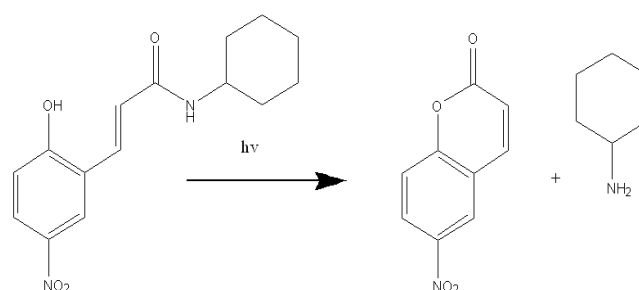


Figure 29 Molecular structure and photoreaction of photobase

minute FRET overlap with PPE (Figure 30) and is irreversible, making it a less-than-ideal candidate for this system, but photobase molecules appear to be remarkably rare in comparison to photoacids. Like the photoacid dyes, this molecule is not soluble in water, so the nanoparticle is a necessary vehicle for it to be utilized in aqueous environments.

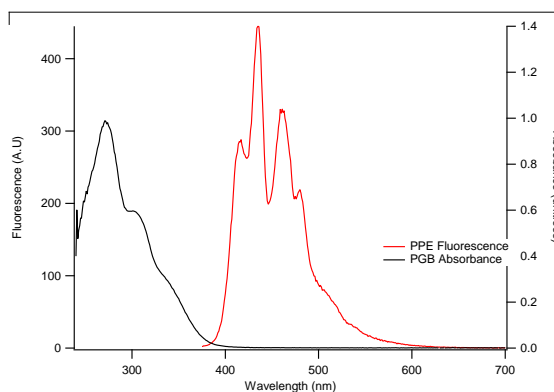


Figure 30 FRET overlap of photobase absorption and PPE fluorescence

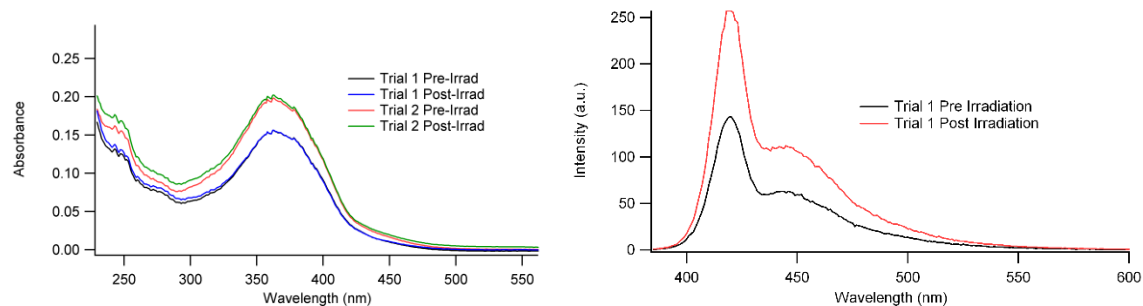


Figure 31 Effect of irradiation on photobase-doped CPNs

Ultimately, this experiment had to be abandoned. I never observed base release with these nanoparticles. Instead, either the pH did not change at all upon irradiation, or actually became slightly more acidic. This, in addition to unexplained increases in absorbance upon irradiation such as is seen in Figure 31, made it clear that some undesirable phenomena were occurring that we could neither predict nor prevent. I do believe that after recent advances with the acid release project, this base release branch deserves to be revisited.

Appendix 3 PVK Nanoparticles

Soon after I joined the lab, Christian decided to try a different acid-releasing FRET pair. Together, we tested nanoparticles made from conjugated polymer PVK (refer back to Figure 1 for structure) and the irreversible photoacid 2-nitrobenzaldehyde (Figure 32). The goal was to overwhelm the polymer's ability to absorb acidic protons by using an irreversible dye.

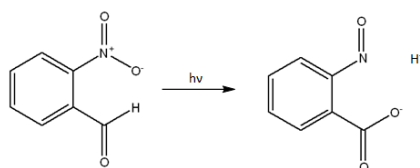


Figure 32 Nitrobenzaldehyde Structure

This experiment proved successful. We observed an average pH drop of .20 units in multiple trials and fluorescence increased, as would be consistent with the occurrence of FRET. However, PVK required irradiation at 254nm to be excited, which is too high in energy for use in most biological

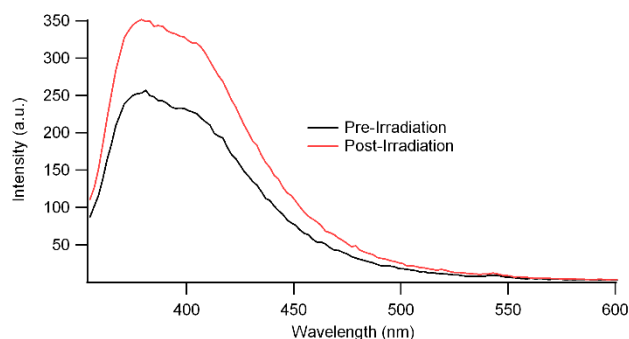


Figure 33 Fluorescence of PVK CPNs

applications. Additionally, the lack of reversibility meant that these nanoparticles would not be useful to finetune the pH of a system, as was the project's original goal. It is possible, however, that novel research can still be achieved with this system, or one like it.

Appendix 4 Synthesis

All chemicals but the photoacid and photobase dyes were purchased from Acros or Sigma Aldrich and used as received unless otherwise specified.

THOMeCl₃ was prepared following a literature procedure¹³. 0.6647 g *p*-anisidine + 2 mL concentrated HCl in 2 mL of DI water cool in ice bath. Solution turned purple and precipitate formed upon addition of the acid. Sonicated 1min to fully dissolve. Separate solution of .4152 g of Sodium Nitrite +5 mL DI water was cooled in ice bath. I added the sodium nitrite solution dropwise over 15 min to the *p*-anisidine solution, while keeping the temperature below 5°C. End solution was a brown color with a yellow tinge. Separate solution of 1.067 g of 2,4,5 trichlorophenol + 1.064 g NaOH + 10 mL DI water was cooled in ice bath. Sonicated to dissolve everything. Solution was a cloudy white. The *p*-anisidine solution was added dropwise to the 2,4,5 trichlorophenol solution over 55min. Solution temperature was kept below 5°C. End solution was a cloudy dark red. Stirred 1 hour in ice bath. Vacuum filtered to get a brown paste. High vacuum to remove any water in the sample. Recrystallized in EtOH to get a tan/brown powder. NMR spectrum found below.

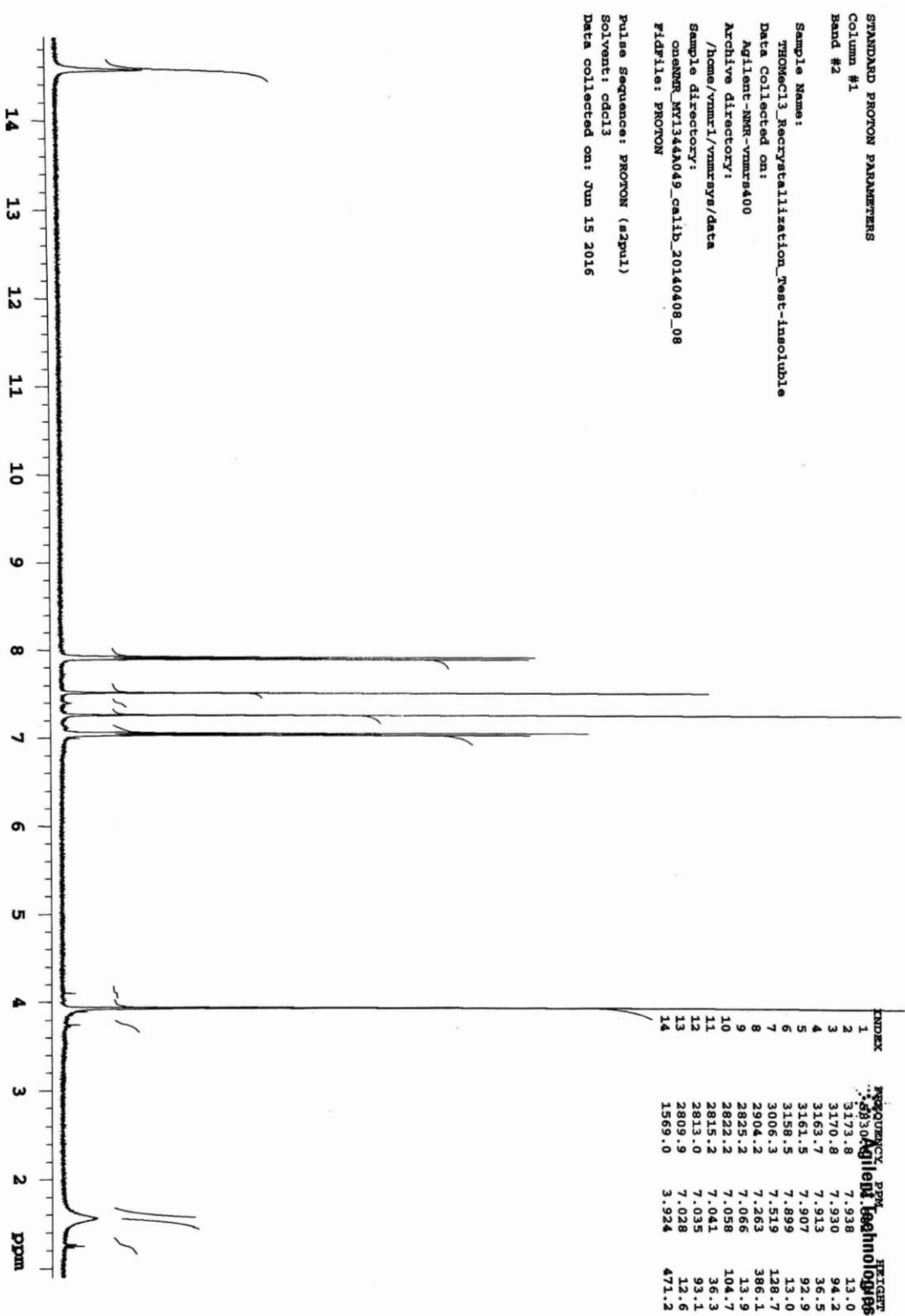
THSMCl₃ was prepared following a very similar literature procedure¹³. 0.7604g 4-(methylthio)aniline + 2ml concentrated HCl in 2mL of DI water was cooled in ice bath. Solution precipitated purple solid upon addition of the acid. Sonicated for 3min to partially dissolve. Cooled in ice bath. Separate solution of .4180g of Sodium Nitrite +5ml DI water sonicated for 1min to dissolved, then cooled in ice bath. Added the sodium nitrite solution to the 4-

(methylthio)aniline solution dropwise over 35min. Solution became black with a yellow tinge. Separate solution of 1.061g of 2,4,5 trichlorophenol + .4602g NaOH + 4.5mL DI water cooled in ice bath. Sonicated to dissolve everything. Solution was a cloudy white. The aniline solution was added dropwise to the 2,4,5 trichlorophenol solution over 90min. Solution temperature was kept below 5°C via ice bath and direct addition of 2g of ice. Solution became a cloudy dark orange. Stirred 40min in ice bath. Filtered to get a brown powder. High vacuum used to remove any water in the sample. Recrystallized in EtOH to get a red/orange powder. NMR spectrum below.

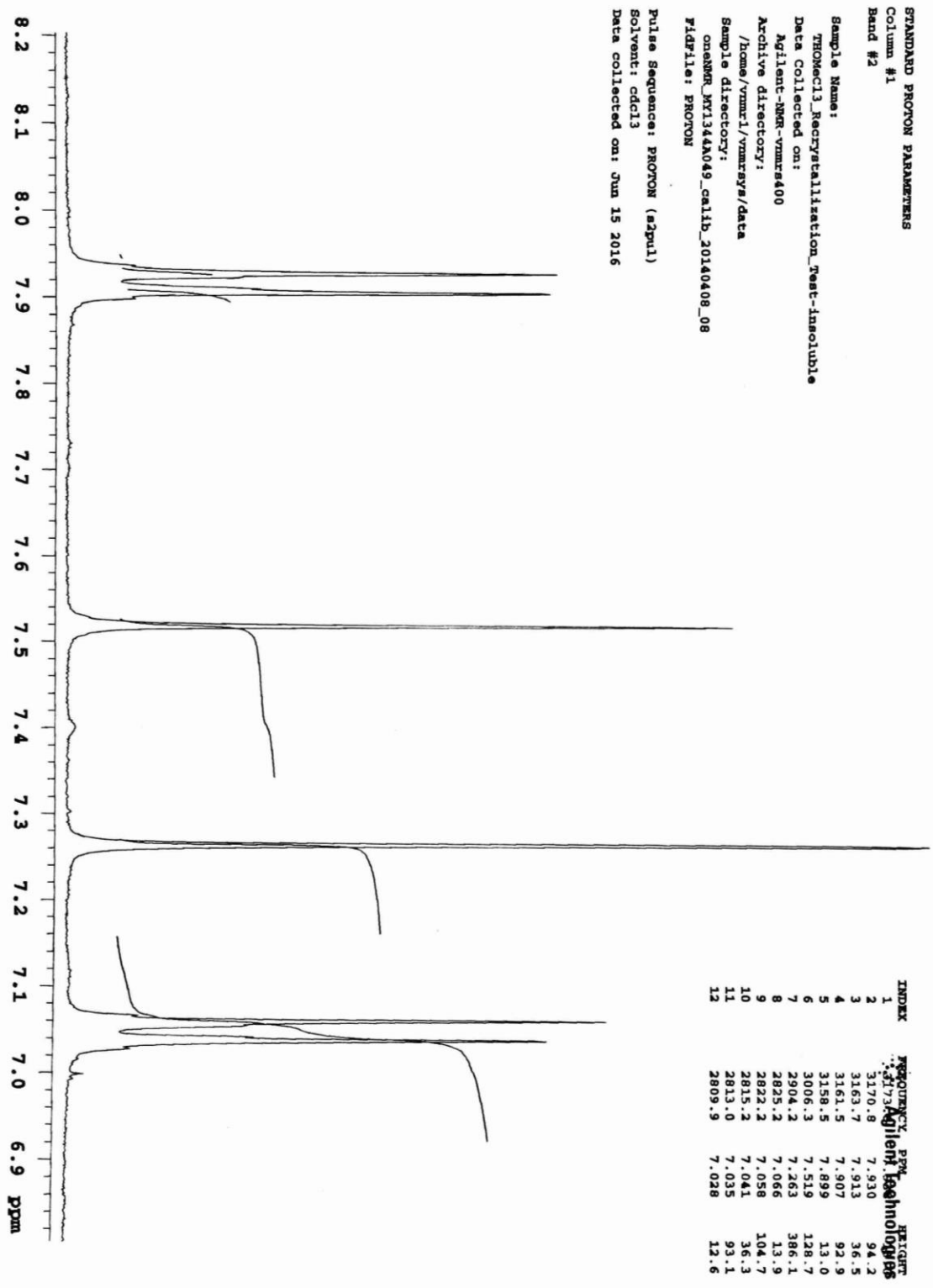
The photobase dye, (E)-N-cyclohexyl-3-(2-hydroxy-5-nitrophenyl)acrylamide, was prepared following a literature procedure¹⁴. 1.5009g 6-nitrocoumarin + 7.5mL cyclohexylamine. Reflux overnight under argon atmosphere. Poured the solution into a beaker containing 20ml of 3.5M HCl and 20ml of CHCl₃. The water turned cloudy white and the solution started smoking. Stirred the solution, the water turned clear and the CHCl₃ turned a cloudy gray color. Filtered the solution to get a solid white/yellow impure product. CHCl₃ filtrate is a clear amber color (this is the unreacted cyclohexylamine). The product was washed with THF followed by a recrystallization in acetone (100ml). Used high vacuum to remove any remaining acetone.

¹H NMR: 1.71–2.09 (10H, m, cyclohexyl), 3.80 (1H, m, –N–CH<), 6.71 (1H, d, *J* = 16 Hz, ArCH=CH–), 6.82–7.20 (4H, m, aromatic), 7.46 (1H, dd, *J* = 1.5, 7.7 Hz, –NH–), 7.85 (1H, d, *J* = 16 Hz, ArCH=CH–), 8.96 (1H, s, –OH),

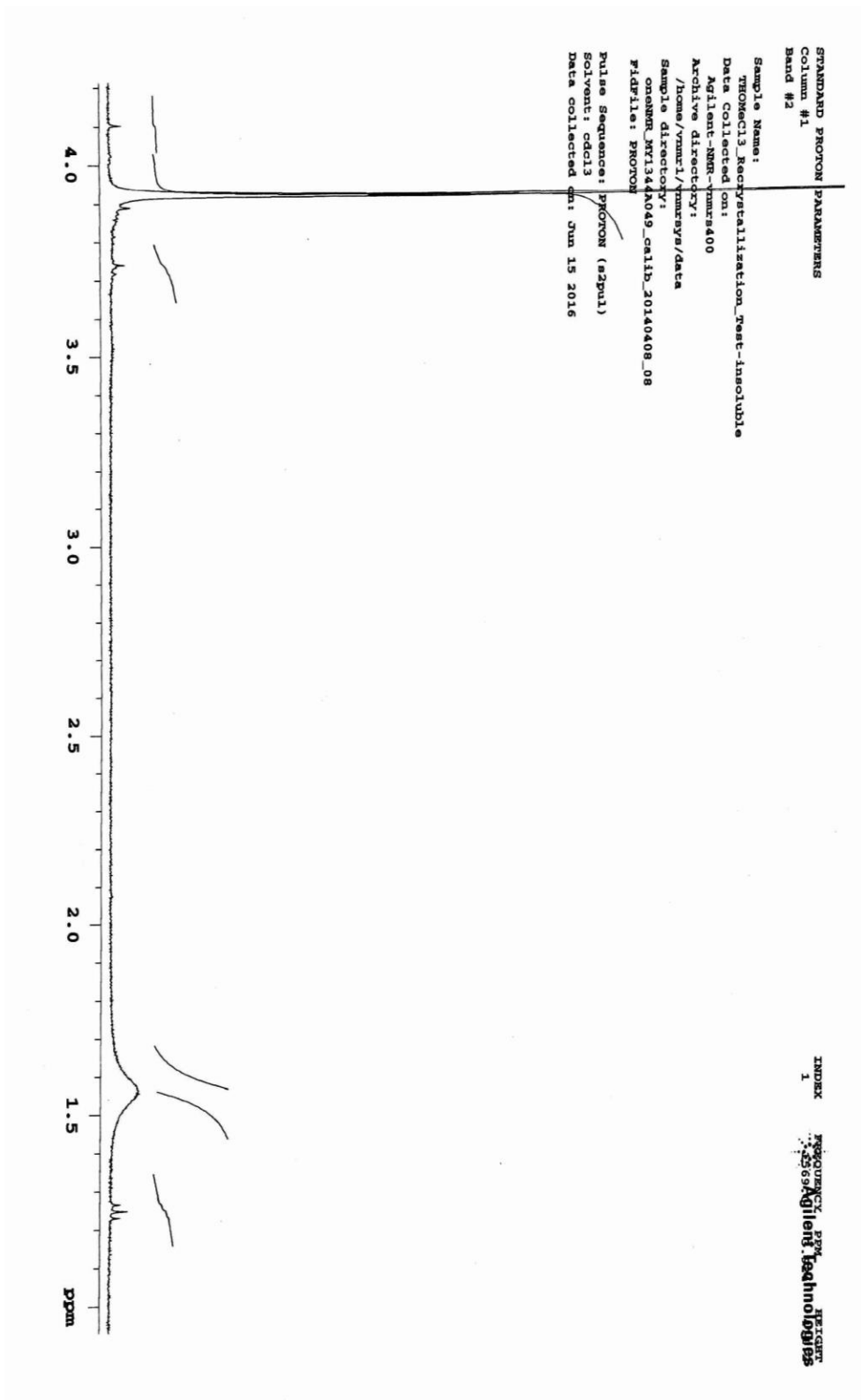
¹H NMR of THOMeCl₃ (full):



¹H NMR of THOMeCl₃ (aromatic):

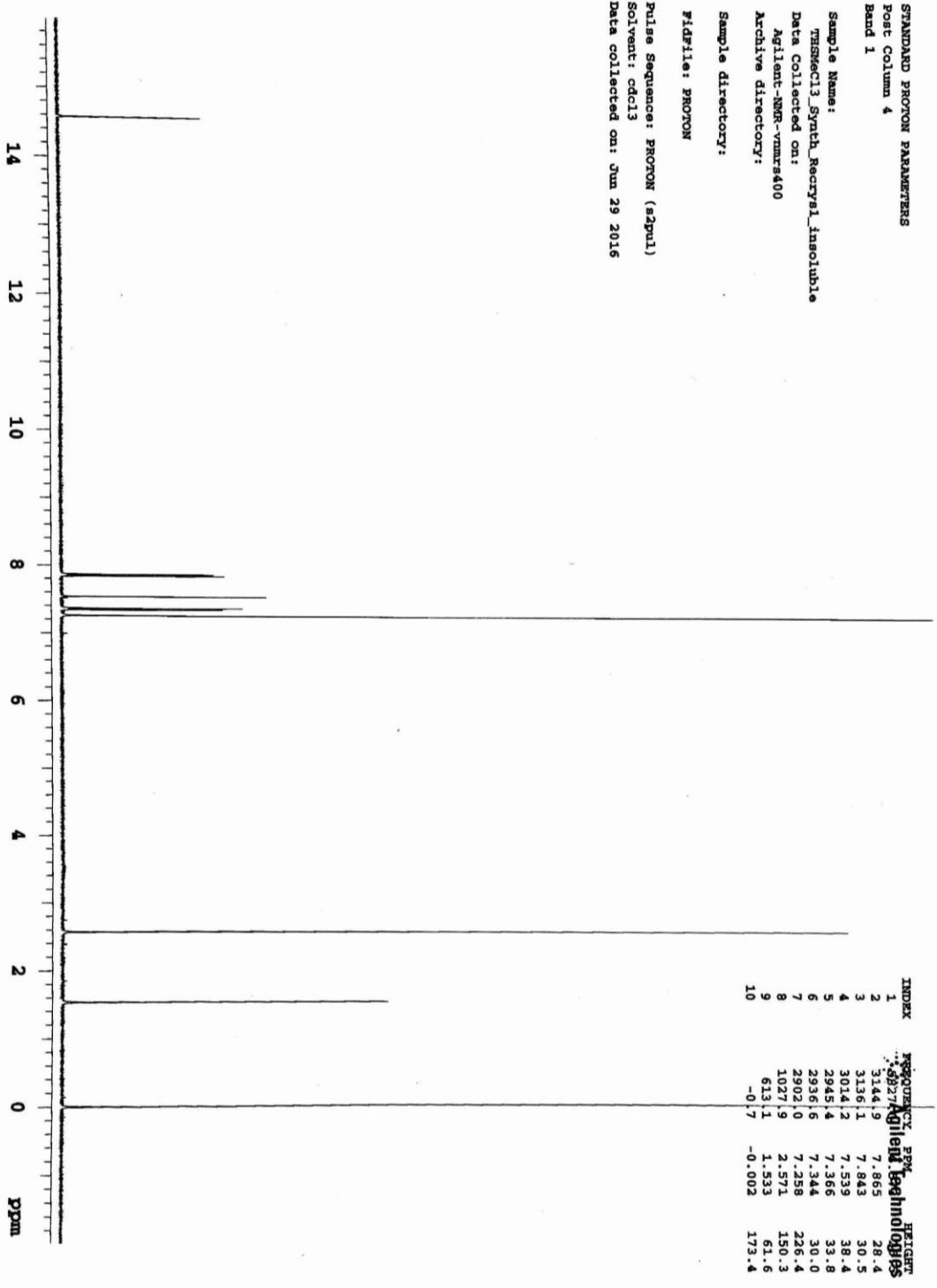


^1H NMR of THOMeCl_3 (aliphatic):



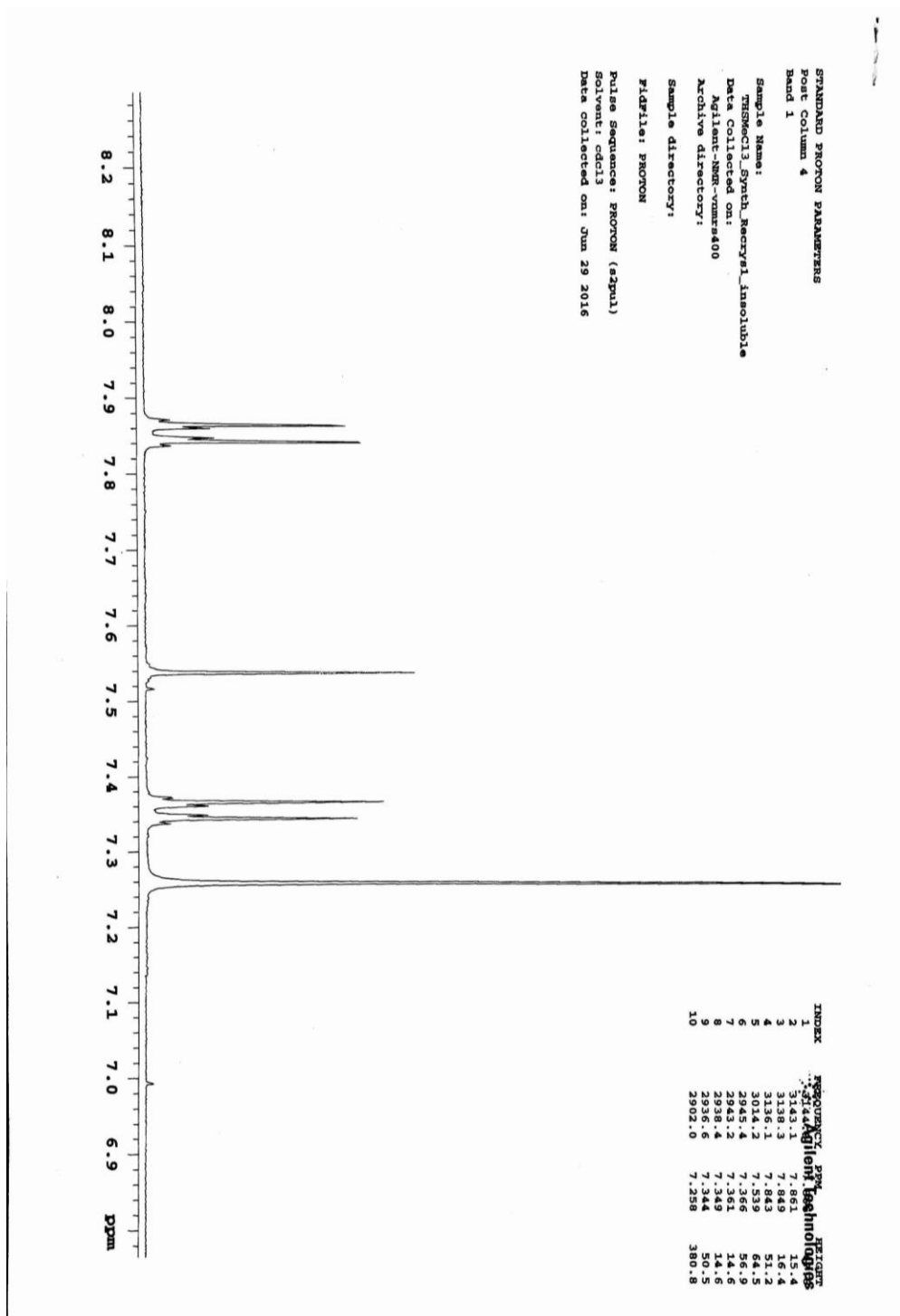
¹H NMR of THSMcCl₃ (full):

21b06291661

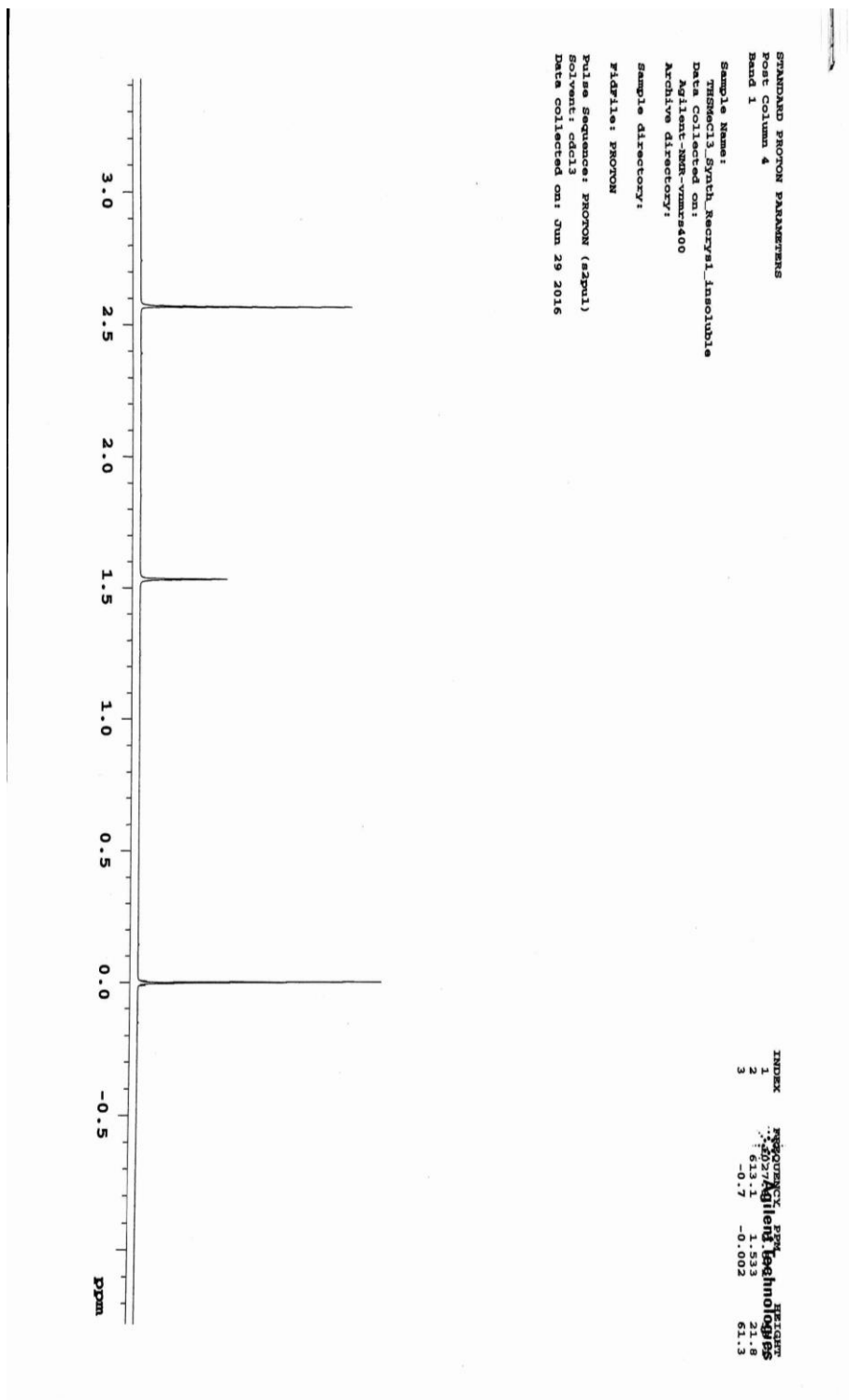


STANDARD PROTON PARAMETERS
 Post Column 4
 Band 1
 Sample Name:
 THSMcCl₃ Synth Recryst Insoluble
 Data Collected on:
 Agilent-NMR-vnmr400
 Archive directory:
 Sample directory:
 FIDFile: PROTON
 Pulse Sequence: PROTON (s2pul)
 Solvent: cdcl3
 Data collected on: Jun 29 2016

¹H NMR of THSMcCl₃ (aromatic):



^1H NMR of THSMeCl_3 (aliphatic):



-
- ¹ Wu, C., Bull, B., Szymanski, C., Christensen, K., & McNeill, J. (2008). Multicolor conjugated polymer dots for biological fluorescence imaging. *ACS Nano*, 2(11), 2415-23.
- ² Dickenson, N., & Picking, W. (2012). Förster Resonance Energy Transfer (FRET) as a Tool for Dissecting the Molecular Mechanisms for Maturation of the Shigella Type III Secretion Needle Tip Complex. *International Journal of Molecular Sciences.*, 13(12), 15137-15161.
- ³ Johns VKK. Visible-light-responsive reversible photoacid based on a metastable carbanion. *Chem - Eur J* 2014 -01;20(3):689-692.
- ⁴ Luo Y, Wang C, Peng P, Hossain M, Jiang T, Fu W, Liao Y, Su M. Visible light mediated killing of multidrug-resistant bacteria using photoacids. *J Mater Chem B* 2013;1(7):997-1001.
- ⁵ Maity C. Spatial structuring of a supramolecular hydrogel by using a visible-light triggered catalyst. *Angew Chem , Int Ed* 2015 -01;54(3):998-1001.
- ⁶ Allen RMM. Microbial fuel-cells electricity production from carbohydrates. *Appl Biochem Biotechnol* 1993;39-40(1):27-40.
- ⁷ Chen Y. DNA nanotechnology from the test tube to the cell. *Nat Nanotechnol* 2015;10(9):748-760.
- ⁸ Wu, C., Bull, B., Szymanski, C., Christensen, K., & McNeill, J. (2008). Multicolor conjugated polymer dots for biological fluorescence imaging. *ACS Nano*, 2(11), 2415-23.
- ⁹ Emond M. 2-hydroxyazobenzenes to tailor pH pulses and oscillations with light. *Chem - Eur J* 2010 -08;16(29):8822-8831.
- ¹⁰ Bhattacharyya, S., Barman, M., Baidya, A., & Patra, A. (2014). Singlet Oxygen Generation from Polymer Nanoparticles-Photosensitizer Conjugates Using FRET Cascade. *Journal of Physical Chemistry C*, 118(18), 9733-9740.
- ¹¹ Caruso, F. Influence of Polyelectrolyte Multilayer Coatings on Förster Resonance Energy Transfer between 6-Carboxyfluorescein and Rhodamine B-Labeled Particles in Aqueous Solutions. *J. Phys. Chem. B*, 1998, 102 (11), pp 2011-2016
- ^{12,14} Arimitsu, K., Takemori, Y., Nakajima, A., Oguri, A., Furutani, M., Gunji, T., & Abe, Y. (2015). Photobase generators derived from *trans-o*-coumaric acid for anionic UV curing systems without gas generation. *Journal of Polymer Science.*, 53(10), 1174-1177.
- ^{13,13} Photoinduced pH drops in Water; Mattieu Emond et al. *Phys. Chem. Chem. Phys.*, 2011, 13 6493-6499